

# Experimental Study on the Performance of Slope-crested Groynes in Erodible Meandering Channels of Different Sinuosity

---

Saroj KARKI<sup>1</sup>, Hajime NAKAGAWA<sup>2</sup>, Kenji KAWAIKE<sup>3</sup> and Masakazu HASHIMOTO<sup>4</sup>

---

## Experimental Study on the Performance of Slope-crested Groynes in Erodible Meandering Channels of Different Sinuosity

Saroj KARKI<sup>1</sup>, Hajime NAKAGAWA<sup>2</sup>,  
Kenji KAWAIKE<sup>3</sup> and Masakazu HASHIMOTO<sup>4</sup>

### Abstract

Riverbank erosion is a vital issue in the management and restoration of rivers, especially in alluvial meandering channels because of their unique channel morpho-dynamics. Various countermeasures are thus implemented to minimize riverbank erosion and maintain stable channel sections of meandering channels. This study analyzes the performance of modified impermeable groynes with sloped crests as a countermeasure for bank erosion. Experiments were conducted in erodible meandering channels of two different sinuosities to evaluate the performance of the proposed countermeasures under varying sinuosity as well as analyze the overall morphological evolution of the channel. The results show that the low sinuosity (LS) channel was more prone to erosion compared to the higher sinuosity (HS) channel. Channel sinuosity also affected the overall channel morphological evolution with the LS channel showing more distinct characteristics of a meandering channel forming point bar and pool and riffle sequences. The proposed countermeasure showed slightly better performance in the case of the LS channel. Although the presence of the proposed groynes did not significantly deflect the high-velocity core towards the channel center, the velocity near the bank region was significantly reduced.

Key words : Meandering channel, Sinuosity, Bank erosion, Groyne.

---

<sup>1</sup> Doctoral Student, Dept. of Civil and Earth Resources Engineering, Kyoto University, Japan

<sup>2</sup> Prof., Disaster Prevention Research Institute (DPRI), Kyoto University, Japan

<sup>3</sup> Assoc. Prof., DPRI, Kyoto University, Japan

<sup>4</sup> Asst. Prof., IRIDeS, Tohoku University, Japan

## 1. INTRODUCTION

It is important to protect river banks from erosion, particularly in meandering channels, in order to maintain the stable dimensions, patterns and profile of a river (Bhuiyan et al., 2010). Based on previous studies as well as observation in natural channels, erosion occurs at the outer bank forming deep pools and deposition occurs at the inner bank forming a point bar (Struiksma et al., 1985; Hickin and Nanson, 1984). Erosion-deposition induced channel migration in meandering rivers causes the loss of hundreds of hectares of mainland floodplain and agriculture, affecting the livelihood of millions of people around the world. Such phenomena have inspired the search for different bank protection countermeasures to improve outer bank stability and minimize erosion (Cunningham and Lyn, 2016). Although bank protection countermeasures such as submerged vanes, bendway weirs, stream barbs, bank-attached vanes, bandal like structures, etc. have been tested (Jamieson et al., 2013; Bhui-

yan et al., 2010; Teraguchi et al., 2011; Cunningham and Lyn, 2016), groynes are still one of the most widely implemented countermeasures for bank protection especially in natural bends or meandering channels (Teraguchi, 2011). Groynes help to protect the riverbank from erosion by deflecting high-velocity flow away from the banks to the channel center (Uijtewaal, 2005; Dehghani et al., 2013). However, rectangular impermeable groynes can cause increased flow velocity and result in increased erosion on the opposite bank, high turbulence and vorticity behind the structures and high scour near the tip of structures (Zhang and Nakagawa, 2009; Karki et al., 2018; Zhang et al., 2009; Dehghani et al., 2013). **Figure 1** shows time series images of the impact of rectangular impermeable groynes on the erosion-deposition process in the bend of an alluvial river. Due to the deposition induced by the groyne field, a significant portion of land has been reclaimed on the adjacent bank. However, nearly the same amount of land has been

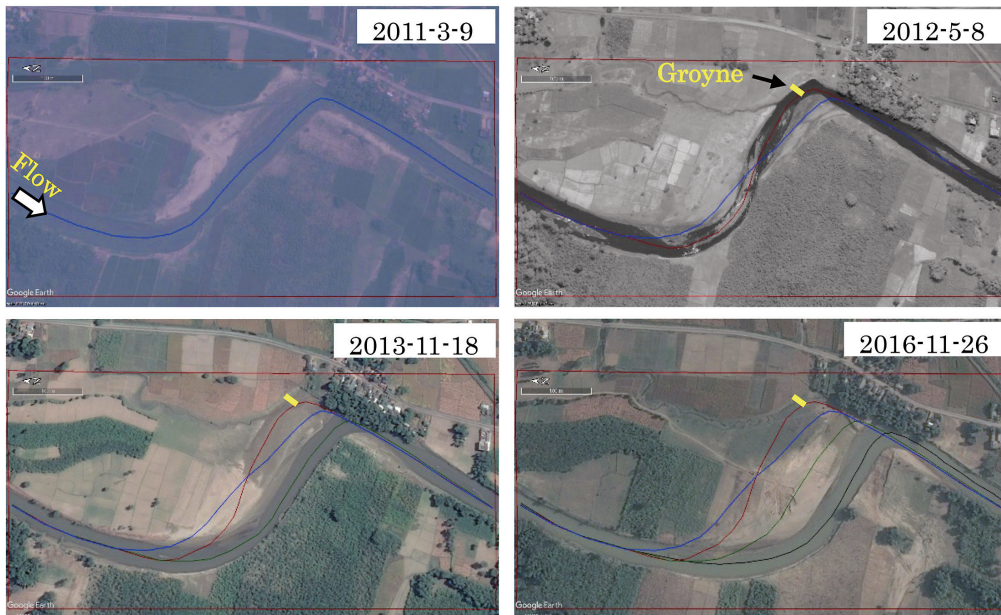


**Fig. 1** Time series images of the channel planform evolution after implementation of a groyne. (Google Earth, 2018)

lost to erosion on the opposite bank. In order to minimize such adverse impacts, the shape and orientation of the structures have been modified by changing the shape of the tip of the groynes (L-head, T-head, round head, etc.), varying the angle of inclination, adjusting the permeability of the structure, and changing the slope of the crest of groynes.

Various experimental studies have examined the effect of groynes on the flow field, local scour, sediment transport, channel evolution, etc. However, most of those studies on countermeasures such as groynes have been performed in straight channels (Zhang and Nakagawa, 2009; Yossef and Vriend, 2010; Uijttewaal, 2005). Even in cases of meandering channels, most of the previous studies considered either a fixed bed and fixed bank (FBFB) or an erodible bed and fixed bank (EBFB) channels (Giri et. al., 2003; Giri and Shimizu, 2004). Moreover, such experiments focused only on a single channel bend or meandering channel with single sinuosity. Since meandering channels have various characteristics (sinuosity, amplitude, deflection angle, ratio of radius of curvature to the channel width (R/B), etc.), the effectiveness of countermeasures cannot be fully evaluated under a single sinuosity channel as it can be affected by dominant channel characteristics. Studies related

to the effect of sinuosity in sine-generated (SG) meandering channels have been conducted to understand the flow dynamics and channel morphological evolution (Da Silva et al., 2006; Xu and Bai, 2012). However, studies considering the effect of channel sinuosity on the performance of bank protection countermeasures have not been tested. The current study investigated the performance of slope crested impermeable groynes in erodible meandering channels of two different sinuosities.

## 2. EXPERIMENTAL SET-UP

### 2.1 Meandering Channel Preparation

The experimental works discussed in the current study were conducted in Ujigawa Open Laboratory under the Disaster Prevention Research Institute (DPRI), Kyoto University. The schematic layout of the experimental flume as illustrated in Fig. 2 consists of a fixed bed inlet and outlet channel 50 cm and 100 cm in length, respectively. The main channel includes a 400 cm long and 200 cm wide erodible bed filled with non-uniform ( $D_{\text{mean}} = 0.72 \text{ mm}$ ,  $\sigma = (d_{84}/d_{16})^{0.5} = 1.38$  and specific gravity = 1.41) and non-cohesive sediment up to a thickness of 20 cm from the bottom. The sine-generated curve (SGC) defined by Eq. (1) was used to delineate the meandering channels within the erodible boundary. The main parameters determining the

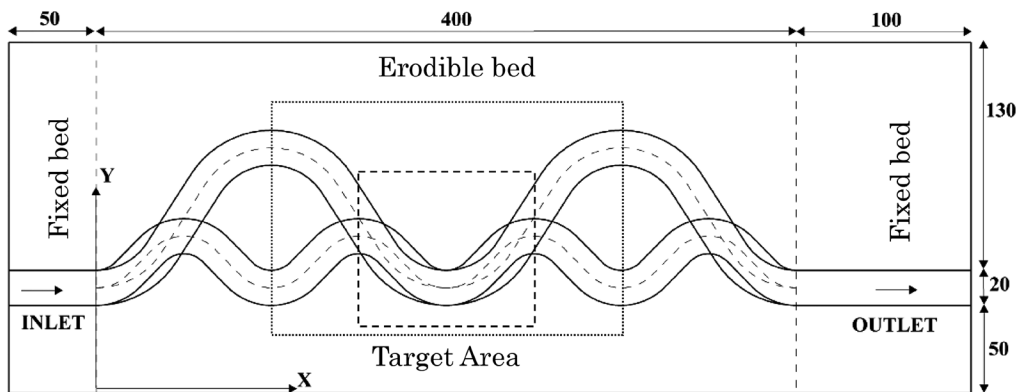


Fig. 2 Schematic layout of the two experimental channels used in the study (units in centimeters)

SGC are channel-wise wavelength ( $M$ ) and maximum deflection angle ( $\omega$ ) (Langbein and Leopold, 1966).

$$\phi = \omega \cdot \cos\left(2\pi \frac{s}{M}\right) \quad (1)$$

where  $s$  is the channel-wise length and  $\phi$  is the local deflection angle.

By integrating Eq. (1) in the X- and Y-direction, valley-wise wavelength ( $\lambda$ ) and amplitude ( $A$ ) were obtained. In this experiment, two SG channels were prepared whose different parameter values are listed in **Table 1**.

To prepare an erodible meandering channel, first, the channel bed was compacted and levelled, then bank materials around were filled and compacted around a prefabricated wooden channel. Two separate prefabricated wooden channels following a SGC were constructed to prepare experimental meandering channels of two different sinuosities. The same type of sediment was used in the bed as well as in the bank. After the bank materials were compacted and levelled, the prefabricated channel was carefully removed to obtain the designed rectangular experimental channel having an initial width of 20 cm and depth of 5 cm. The same procedure was repeated to prepare both types of channels.

## 2.2 Experimental Methods

A series of experiments were conducted under two different channels to ensure that the results

were generalized and a total of four experiments were selected for this study, i.e. two experiments for each type of meandering channel. For each meandering channel, one experiment without any countermeasures and another experiment with countermeasures were performed. The four cases in this study were a high sinuosity channel without groynes (HS-NG) and with groynes (HS-G), and a low sinuosity channel without groynes (LS-NG) and with groynes (LS-G). The experimental flow conditions are presented in **Table 2**.

The experimental flow was partially governed by the size of the channel as well as non-cohesive sediments used for making the erodible channel. Preparing a larger channel would have been extremely difficult. Also, due to the non-cohesive sediments, the selection of a higher discharge would have resulted in high and rapid erosion forcing us to shorten the experimental time. A discharge was chosen that transports sediment but does not overtop the banks of the designed channel. Experiments were conducted under clear water conditions for a duration of 40 minutes (mins). In the cases of experiments with countermeasures, for the first 20 mins, the channel was allowed to adjust to the flow conditions. The flow was then stopped, the countermeasures were installed along the pre-determined locations along the outer bank and then the flow was resumed for the next 20 mins. In both cases, a constant discharge of 0.95 l/s was supplied by a pump to the upstream storage tank through which water gradually entered the

**Table 1** Parameters of Experimental Channels

Parameter (cm)	Channel-LS	Channel-HS
Width (B)	20	20
Radius of Curvature (R)	25	45
R/B Ratio	1.25	2.25
Amplitude (A)	30	80
Meander Length (L)	120	270
Valley Wavelength ( $\lambda$ )	100	200
Sinuosity ( $K = L/\lambda$ )	1.2	1.35
Angle of Deflection ( $\omega$ )	45°	60°

**Table 2** Experimental Flow Conditions

Flow Variable	Value
Discharge (l/s)	0.95
Mean Flow Depth (cm)	2.86
Mean Velocity (cm/s)	16.6
Channel Slope	1 :550
Shear Velocity (cm/s)	1.99
Froude Number	0.31
Reynolds Number	5322

channel inlet. The target area for the study in the case of both channels is shown in Fig. 2.

Various parameters of the flow and channel, namely: surface velocity distribution, water-level at particular locations and bed topography were measured every 20 mins during the experiments. For the determination of the surface flow field, polyvinyl chloride (PVC) particles having a mean diameter of  $50\ \mu\text{m}$  were used as trace particles while the analysis was performed using MATLAB software. Channel topography was measured using a laser displacement sensor.

### 2.3 Arrangement of Groynes

Groynes modified for the present studies consisted of a triangular portion inclined from the bank top towards the channel and a rectangular portion inserted inside the banks to prevent the flow outflanking around the structures. Compared to the rectangular groynes, the sloping crest from the bank towards the channel caused minimum flow constriction, less turbulence and safe passage

of flow. The dimensions and a schematic layout of the groynes are shown in Fig. 3.

The position of the groynes along the outer bank is shown in Fig. 4 for both channels. Groynes are placed starting from upstream of the apex to the crossover or the point of inflection along the outer bank. Accordingly, due to the difference in channel length, the number of groynes in each type of channel varied from one to another. The groynes from upstream up to the apex were inclined at  $120^\circ$  to the upstream bank in order to ensure a smooth flow approach towards the downstream groynes whereas the groynes downstream of the apex were placed at right angles to the bankline. During the

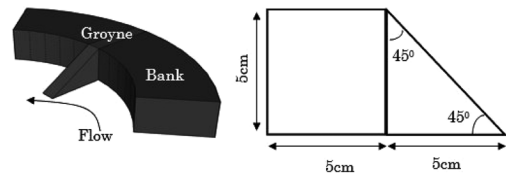


Fig. 3 Schematic layout and geometry of the groynes

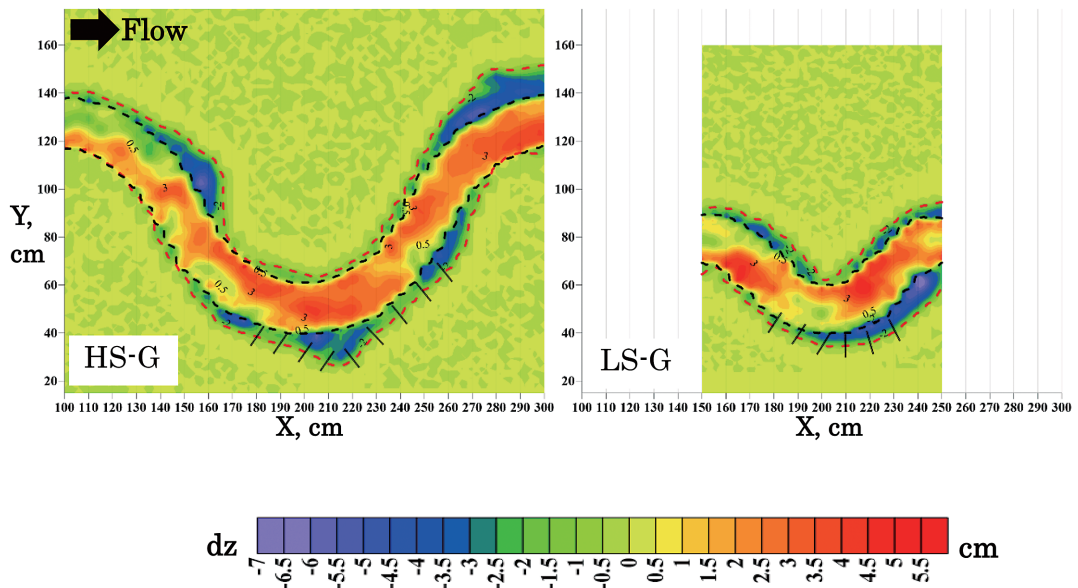


Fig. 4 Position of the groynes and the change in the channel bed elevation between time,  $t=20$  mins and  $t=0$  mins for cases HS-G and LS-G.



initial channel adjustment period, the pattern, location and the extent of the bank erosion varied from one channel to another as shown by the change in channel elevation ( $dZ = Z_{20 \text{ mins}} - Z_{0 \text{ mins}}$ ) between  $t = 20$  mins and  $t = 0$  mins in Fig. 4. Due to this non-uniformity in the bank erosion process, the positioning of the groynes was also affected. The bank erosion process after the implementation of groynes is discussed in the next section.

### 3. RESULTS AND DISCUSSION

#### 3.1 Morphological Evolution of the Channel

The morphology of a meandering channel continuously evolves due to the interaction of flow, sediment transport and channel planform. Figure 5 (a-d) shows the difference ( $dZ = Z_{40 \text{ mins}} - Z_{0 \text{ mins}}$ ) in channel elevation between the end ( $t = 40$  mins) and the start ( $t = 0$  mins) of the experiment for all cases (the flow is from the left to the right). The black dashed line in the figure represents the original bankline ( $t = 0$  mins) while the red dashed line indicates the bankline at the end of the 20-minute

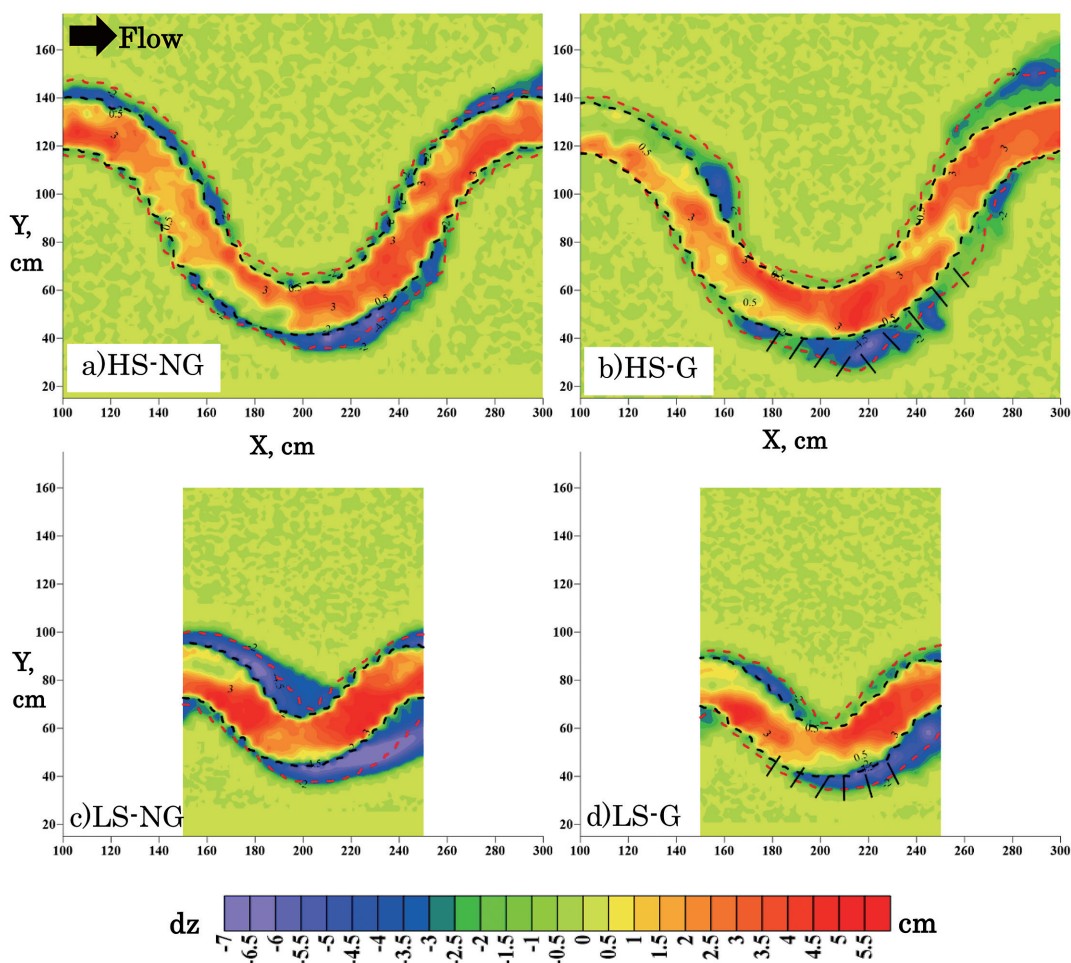


Fig. 5 (a-d): Change in the channel bed elevation between the final ( $t = 40$  mins) and the initial ( $t = 0$  mins) time for all experiment cases.

experiment, just at the time of implementation of the groynes. Positive values in the figure signify deposition while negative values indicate erosion. In both channels, at the beginning of the experiment, the erosion at the bank toe caused the bank materials to fail as a block mass, which was transported by the flow. In the later stages, the bank slope adjusted to the flow conditions and thus mass failure did not occur. However, due to excess near-bank shear stress, fluvial erosion continued at specific locations along the channel banks resulting in the widening of the channel. The erosion rate was higher in the case of LS-NG compared to that of HS-NG. In the cases of the high sinuosity channel (HS-NG and HS-G), the characteristic features of a meandering channel such as a pool and riffle sequence did not distinctly develop as compared to the cases of the low sinuosity channel (LS-NG and LS-G). This difference could be attributed to the unequal erosion in the HS and LS channel. Since no sediment was supplied externally, all the transport of sediment must occur from the bed and the bank materials. Accordingly, the higher erosion in the LS-channel resulted in more transport of sediment to develop deep pools and the subsequent point bar on the opposite bank. The growth of the point bar and the consequent migration of deep pools towards the outer bank resulted in higher erosion in the cases of LS-NG and LS-G. However, in the case of HS-NG and HS-G, the size of the deep pools, as well as the point bar, were comparatively smaller and there was less overall erosion.

The ratio of the radius of curvature ( $R$ ) of the channel centerline to the channel width ( $W$ ), which signifies the sharpness or the tightness of the channel curve is an important parameter controlling the channel erosion and migration (Hickin and Nanson, 1975) in meandering channels. The HS channel, due to the longer flow path and high value of the  $R/B$  ratio, had smooth flow transition and thus less erosion occurred in the HS-NG case.

However, the LS channel had a shorter channel flow path and low  $R/B$  ratio, which caused rapid flow transition and resulted in higher erosion in the LS-NG case. In the HS-NG case, maximum erosion occurred near the point of inflection or cross-over region whereas in the case of LS-NG, channel erosion occurred near the apex of the inner bend and gradually shifted in the upstream direction. The extent of erosion or channel expansion had an effect on the direction of the flow approach, which in turn dictated the performance of the groynes. The erosion and channel evolution pattern in the case of LS-NG were more uniform and predictable as compared to the HS-NG case. The bed forms including the point bar tended to migrate downstream in both channels.

With the installation of groynes, the erosion near the outer bank apex was controlled in both the HS and LS channels. The erosion at the downstream of the apex was also greatly reduced in the case of LS-G but slightly higher erosion occurred in HS-G. Within the field of the groynes, erosion was minimized, however, it continued on the downstream end after exiting the groynes field. The size of the deep pools as well as the scours at the outer bank in the case of LS-G were also reduced to some extent as compared to those in the LS-NG case. Although scour at the tip of the groynes was observed in one or two groynes, the overall scour at the tip of the groynes was not so significant. Considerable erosion occurred in the space between the groynes in the case of HS-G compared to that of the LS-G. The deep pools in the case of LS-G caused the incoming flow velocity to be more moderate and thus reduced the turbulence whereas in the case of HS-G, the approach on the groynes occurred with higher velocity thereby causing more recirculation behind the groynes. This angle of approach might also be influenced by the deflection angle of the meandering channel since the HS channel had a deflection angle of  $60^\circ$  compared to

the 45° of the LS channel.

### 3.2 Erosion–deposition Pattern

The erosion-deposition pattern of the channel was analyzed in order to determine the sediment transport behavior of the channel. Figure 6 depicts the temporal change in the erosion-deposition volume for all cases of the experiment.

The erosion-deposition volume between the successive time periods was calculated based on the change in measured bed elevation at different time periods. The erosion, as well as deposition volume, was higher in the first 20 mins for all cases as the channel underwent rapid adjustment under the given flow conditions. Although the volume was slightly different even for the same type of channel, the overall initial channel adjustment behavior was similar. After the implementation of groynes, the erosion and deposition volume were significantly reduced in the case of LS-G as compared to that of LS-NG. This suggests that the groynes effectively reduced the erosion and enhanced channel transport capacity. However, in the case of HS-G, the erosion-deposition volume changed little compared to that of the HS-NG case. This might suggest that the channel adjustment process was still active in the HS channel.

Figure 7 (a-d) shows the change in the channel elevation ( $dZ = Z_{40 \text{ mins}} - Z_{20 \text{ mins}}$ ) along the initial

channel centerline as well as along the initial right bankline between time  $t = 40$  mins to  $t = 20$  mins, i.e. after the implementation of groynes. Channel erosion is represented by negative values while deposition is given by positive values. The comparison between the LS-NG and LS-G (Fig. 7(a)) shows that the presence of groynes caused degradation along the right bank due to local scouring particularly downstream of the apex. However, along the channel centerline as shown in Fig. 7(b), the channel was continuously aggraded due to the transport of eroded sediment from the bank towards the center. In the case of the HS channel, the channel aggradation-degradation pattern changed little even in the presence of groynes. Along the right bank, slight deposition occurred upstream of the apex and slight degradation was seen just near the apex region (Fig. 7(c)). A similar pattern of elevation change was also observed along the channel centerline as shown in Fig. 7(d).

### 3.3 Surface Velocity Distribution

The continuous change in the channel planform as well as the channel bed due to erosion-deposition phenomena largely affects the distribution of velocity in both the longitudinal as well as transverse direction. Conversely, velocity distribution dictates the channel morphological evolution. In fact, these phenomena proceed simul-

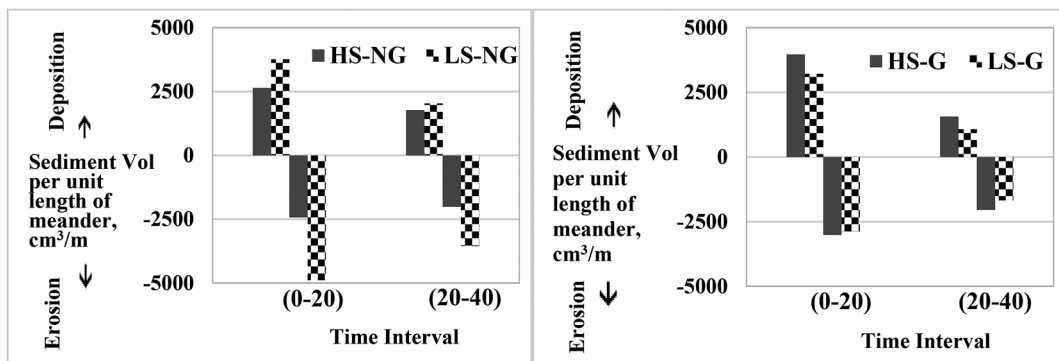


Fig. 6 Temporal change in the erosion–deposition volume for different experiment cases.



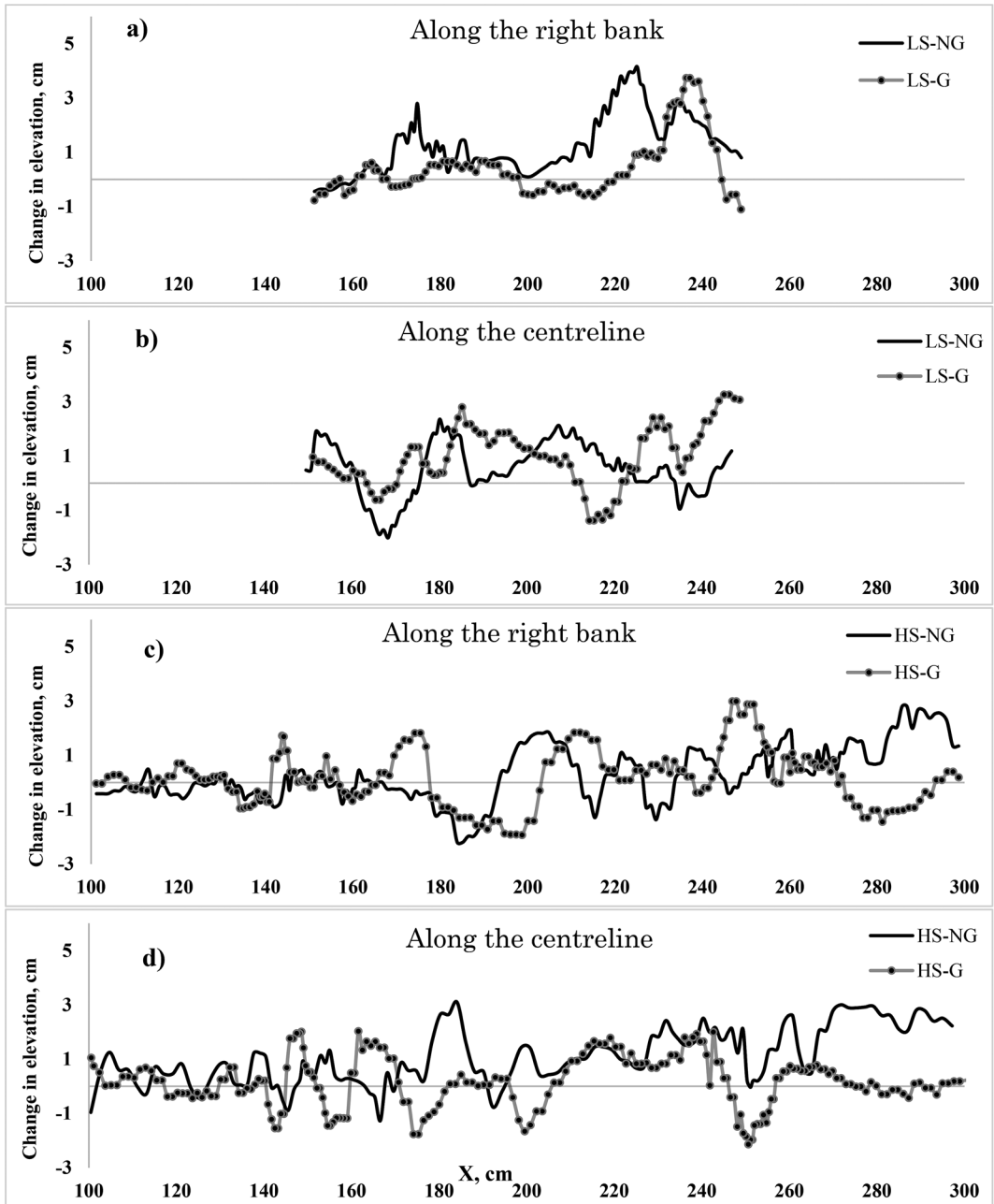
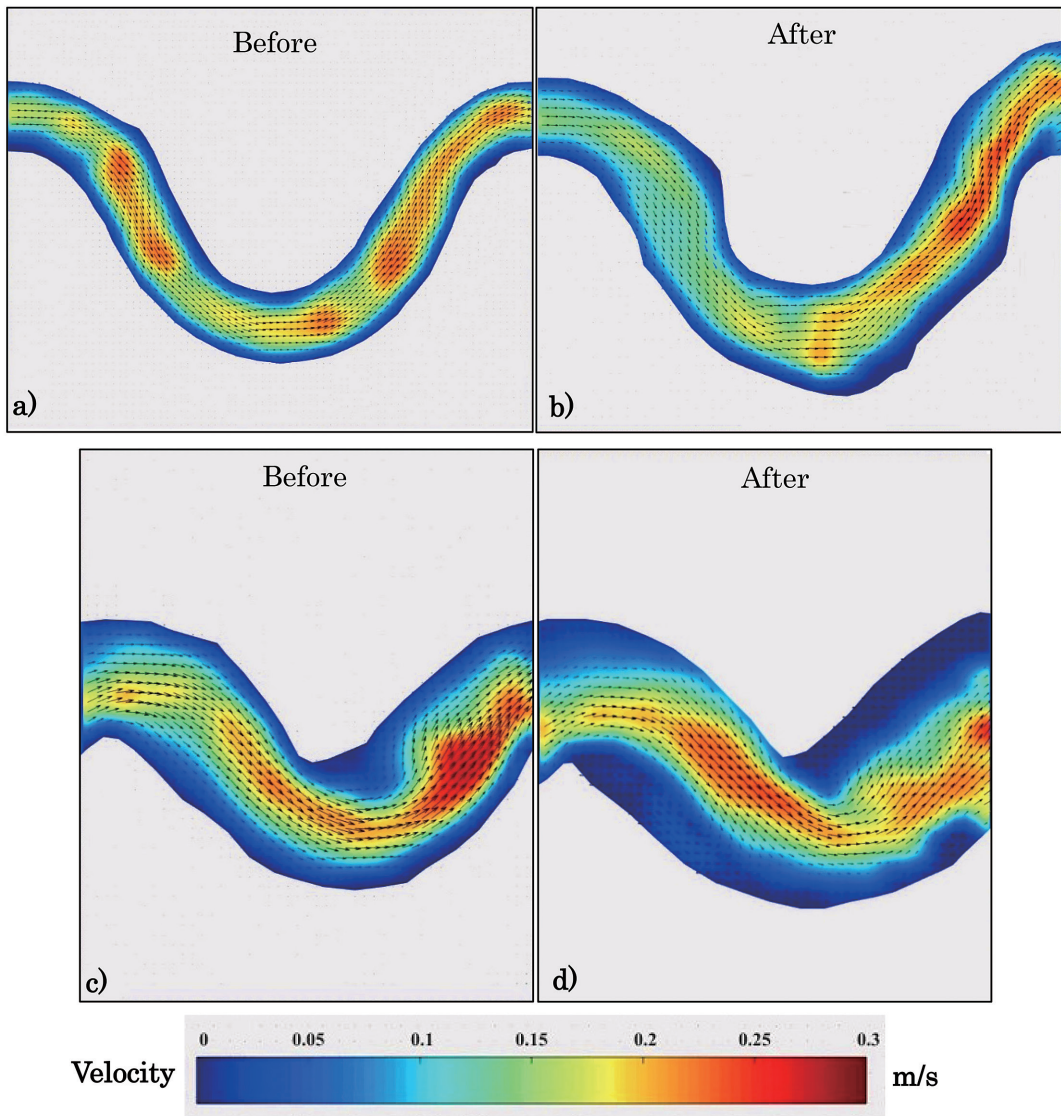


Fig. 7 (a-d): Difference in the elevation between  $t=40$  mins and  $t=20$  mins along the original channel centerline and along the original right bankline.

taneously. Surface velocity distribution obtained by the PIV technique was analyzed to determine how the morphological evolution process is related to the velocity distribution in the channel. **Figure 8** shows the distribution of the surface velocity before implementing the groynes (first 20 mins) and after implementing the groynes (next 20 mins) in the cases of HS-G (**Fig. 8 a and b**) and LS-G (**Fig.**

**8 c and d**).

During the initial 20 mins where the channel adjustment process was dominant, the velocity distribution within the channel was nearly uniform. After the channel adjusted to the given flow conditions by undergoing morphological changes, the distribution of velocity also tends to be non-uniform. Due to the longer flow path as well as the



**Fig. 8** (a-d): Velocity distribution along the channel before (first 20 mins) and after (last 20 mins) implementation of the groynes.

R/B ratio, smooth flow transition occurred in the HS-G case. Consequently, the velocity was more or less uniformly distributed across the channel section as well as along the channel as shown in Fig. 8(a). However, the velocity was slightly high at the point of inflection between the two apices because of which higher erosion was observed around those areas. Similarly, in the case of LS-G, before the implementation of groynes, the high velocity was concentrated near the apex of the inner bend as shown in Fig. 8(c), which caused higher erosion around that region. The transverse velocity component in the case of the LS channel was higher because of which more bed load transport occurred forming deep pools near the outer bank and point bar near the inner bend. After the implementation of the groynes, the near bank velocity was significantly reduced in both LS-G and HS-G (Fig. 8 (b and d)). However, apart from the slight deflection around the groynes region, no noticeable change in velocity distribution within the channel was observed. Velocity around the groynes was reduced but it tends to increase after exiting the groynes field as shown in Fig. 8 (b and d). Some previous studies (Karki et al., 2018) on straight rectangular groynes showed a higher flow deflection, which resulted in higher bank erosion on the opposite bank. In the case of LS-G, a stagnant or dead zone

extending from upstream of the outer bank apex to the inner bend apex was observed (Fig. 8(d)).

Similarly, Fig. 9 (a and b), shows the streamlines and velocity near the groynes area in the case of HS-G and LS-G, respectively. For HS-G, a stagnant zone did not develop upstream of the apex. However, in the space between the groynes downstream of the apex, strong recirculation flow was observed, which resulted in higher erosion in that region. Similarly, the flow deflection around the groynes was slightly higher in the case of the HS channel. This was mainly because of the direction of the approach flow towards the groynes. In the case of HS-G, the erosion in the previous bend ( $X = 150-200$  cm) in Fig. 5(b) was minimum due to which the flow smoothly approached towards the initial groynes. However, in the case of LS-G, due to higher erosion in the preceding bend ( $X = 175-200$  cm) in Fig. 5(d), the flow of approach was towards the end groynes and further downstream. Consequently, less flow deflection, as well as higher erosion downstream of the groynes, was observed.

#### 4. CONCLUSIONS AND RECOMMENDATIONS

We examined the evolution of flow and changes in sediment transport and channel morphology

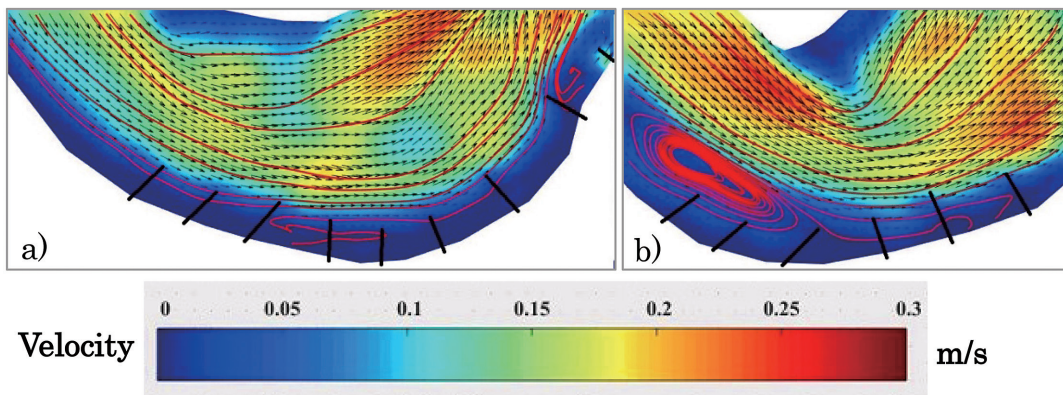


Fig. 9 (a-b): Streamlines and velocity around the groynes: (a) HS-G (b) LS-G

in erodible meandering channels of two different sinuosities. Modified groynes with a sloped crest extending from the bank towards the channel were introduced as a bank protection countermeasure. The effect of the groynes on the evolution of flow and morphology as well as the effect of the channel sinuosity on the performance of the groynes were analyzed. The initial channel adjustment process was similar in both channels but the erosion-deposition pattern was different. Maximum erosion occurred near the inner bend apex in the LS channel whereas in the case of the HS channel, maximum erosion occurred near the point of inflection or the crossover region. The low sinuous channel was characterized by the formation of distinct pool-bar sequences due to higher erosion whereas those features were relatively less distinct in the high sinuous channel. In terms of the bank erosion, again the LS channel was observed to be more prone to erosion under the no groynes case and thus resulted in a uniform widening of the channel. However, in the HS channel, localized bank erosion occurred at some specific points. This suggests that the bank erosion behavior is more difficult to predict in the HS channel, which could ultimately dictate our choice of countermeasures and where to locate them. However, in our experiments, the locations of the groynes were pre-decided. The implementation of a series of groynes influenced the local flow, sediment transport and bank erosion near the structures. Bank erosion was reduced in both types of channel, however, the erosion in between the groynes continued mainly due to recirculation flow and was higher in the HS channel. Although the deflection of high velocity towards the channel center was not significant, the velocity near the bank decreased considerably. After the flow extended beyond the groynes, the velocity increased in both channels. The performance of the proposed countermeasures varied under different sinuosity channels with a slightly better performance in the

case of the LS channel. However, further experiments, as well as numerical simulations under varying flow conditions and different orientations of groynes, are necessary for better understanding of the mechanism.

## ACKNOWLEDGEMENT

This research was supported by the JST/JICA SATREPS program on disaster prevention/mitigation measures against floods and storm surges in Bangladesh (PI: Dr. Hajime Nakagawa). The first author would like to thank the reviewers for their comments to help improve the manuscript and also the Government of Japan for the MEXT scholarship.

## REFERENCES

- Bhuiyan, F., Hey, Richard D. and Wormleaton, Peter R.: Bank-attached vanes for bank erosion control and restoration of river meanders, *Journal of Hydraulic Engineering, ASCE*, Vol. 136, No. 9, pp. 583–596, 2010.
- Cunningham, R.S. and Lyn, D.A.: Laboratory study of bendway weirs as a bank erosion countermeasure, *Journal of Hydraulic Engineering, ASCE*, Vol. 142, No. 6, pp. 1–21, 2016.
- Da Silva, A.M.A., El-Tahawy, T. and Tape, William D.: Variation of flow pattern with sinuosity in sine-generated meandering streams, *Journal of Hydraulic Engineering, ASCE*, Vol. 132, No. 10, pp. 1003–1014, 2006.
- Dehghani, A.A., Azamathulla, H.Md., Hashemi Najafi, S.S. and Ayyoubzaeh, S.A.: Local scouring around L-head groynes, *Journal of Hydrology*, Vol. 504, pp. 125–131, 2013.
- Giri, S., Shimizu, Y. and Fujita, M.: Flow characteristics in a mildly meandering channel with & without river training structures, *Annual Journal of Hydraulic Engineering, JSCE*, Vol. 47, pp. 835–840, 2003.
- Giri, S. and Shimizu, Y.: Observation on bed variation in a meandering like flume with river training structures, *Annual Journal of Hydraulic Engineering, JSCE*, Vol. 48, pp. 1069–1074, 2004.

- Hickin, E.J. and Nanson, G.C.: The character of channel migration on the Beatton River, Northeast British Columbia, Canada, *Geological Society America Bulletin*, Vol. 86, pp. 487-49, 1975.
- Hickin, E.J. and Nanson, G.C.: Lateral migration rates of river bends, *Journal of Hydraulic Engineering*, ASCE, Vol. 110, No. 11, pp. 1557-1567, 1984.
- Jamieson, E.C., Rennie, C.D. and Townsend, R.D.: 3D flow and sediment dynamics in a laboratory channel bend with and without stream barbs, *Journal of Hydraulic Engineering*, ASCE, Vol. 139, No. 2, pp. 154-166, 2013.
- Karki, S., Hasegawa, Y., Hashimoto, M., Nakagawa, H. and Kawaike, K.: Short-term evolution of flow & morphology in an erodible meandering channel with & without groynes, *Annual Journal of Hydraulic Engineering*, JSCE, Vol. 74, No. 4, pp. 1147-1152, 2018.
- Langbein, W.B. and Leopold, L.B.: River Meanders-Theory of minimum variance, *Geological Survey Professional Paper*, Vol. 422-H, pp. H1-H15, 1966.
- Struiksmas, N., Olesen, K.W., Flokstra, C. and Vriend, H.J.D.E.: Bed deformation in curved alluvial channels, *Journal of Hydraulic Research*, Vol. 23, No. 1, pp. 57-79, 1985.
- Teraguchi, H.: Study on hydraulic and morphological characteristics of river channel with groyne structures, PhD Thesis, Kyoto University, 2011.
- Teraguchi, H., Nakagawa, H., Kawaike, K., Baba, Y., and Zhang, H.: Effects of hydraulic structures on river morphological processes, *Int. J. of Sed. Res.*, Vol. 26, No. 3, pp. 283-303, 2011.
- Uijtewaal, Wim S.J.: Effects of groynes on the flow in groyne fields: Laboratory experiments, *Journal of Hydraulic Engineering*, ASCE, Vol. 131, No. 9, pp. 782-791, 2005.
- Xu, D. and Bai, Y.: Experimental study on the bed topography evolution in alluvial meandering rivers with various sinuousnesses, *J. Hydro-environment Research*, Vol. 7, pp. 92-102, 2012.
- Yossef, M. and Vriend, H.D.: Sediment exchange between a river and its groyne fields: mobile-bed experiment, *Journal of Hydraulic Engineering*, ASCE, Vol. 136, No. 9, pp. 610-625, 2010.
- Zhang, H. and Nakagawa, H.: Characteristics of local flow and bed deformation at impermeable and permeable spur dykes, *Annual Journal of Hydraulic Engineering*, JSCE, Vol. 53, pp. 145-150, 2009.
- Zhang, H., Nakagawa, H., Kawaike, K. and Baba, Y.: Experiment and simulation of turbulent flow in local scour around spur dyke, *Int. J. Sed. Res.*, Vol. 24, No. 1, pp. 33-45, 2009.

(投稿受理：平成30年4月6日  
訂正稿受理：平成30年7月4日)

## 要 旨

河岸侵食は河川管理のために重要な課題の一つであり、特に沖積蛇行河川ではその地形動力的な特徴から、重要度が高い。そのため、侵食の最小化や流路の安定化のために、様々な対策が取られている。本研究では斜形不透過型水制の河岸侵食に対する低減効果を分析した。水路実験は、蛇行度の異なる2種類の侵食可能蛇行流路を用いて行った。本研究の目的は、提案する対策の様々な蛇行度における性能を評価することと、流路全体の形態学的な流路の発達を分析することである。結果より、低蛇行度の方が、高蛇行度よりも侵食し易い傾向があることを示した。また、蛇行度は流路全体の形態学的な流路の発達に影響しており、低蛇行度の場合で独特な点状砂州、瀬-淵シーケンスの形成が見られた。提案された対策は低蛇行度の場合で良好な性能を示しており、河岸近傍の流速の低減効果が確認されたが、水はね効果もまた低減されることがわかった。